Journal of Materials Chemistry

Cite this: *J. Mater. Chem.*, 2011, **21**, 14604

www.rsc.org/materials

PAPER

Dibenzothiophene derivatives as host materials for high efficiency in deep blue phosphorescent organic light emitting diodes†

Sook Hee Jeong and Jun Yeob Lee*

Received 30th May 2011, Accepted 12th July 2011
DOI: 10.1039/c1jm12421h

Various dibenzothiophene derivatives were synthesized as high triplet energy host materials for deep blue phosphorescent organic light-emitting diodes (PHOLEDs) and their device performances were investigated. Dibenzothiophene host materials with a hole transport type carbazole and electron transport type phosphine oxide moieties showed high quantum efficiency and low driving voltage due to balanced charge injection and transport. A high quantum efficiency of 20.2% and only 10% reduction of quantum efficiency at 1000 cd m^{-2} were demonstrated from the deep blue PHOLEDs with the dibenzothiophene based high triplet energy host materials.

Introduction

The development of deep blue phosphorescent organic light-emitting diodes (PHOLEDs) is important because they can greatly improve the power consumption of full colour organic light-emitting diode panels. Although a high quantum efficiency was achieved in deep blue PHOLEDs, it is essential to enhance the quantum efficiency of deep blue PHOLEDs.[1] In particular, the quantum efficiency at high luminance should be increased for practical applications.

Most of the studies to improve the quantum efficiency of deep blue PHOLEDs focused on the synthesis of high triplet energy host materials for efficient energy transfer to deep blue phosphorescent dopants.[1–15] Several core structures, such as 9-phenylcarbazole,[1–3] *N*,*N*-dicarbazolyl-3,5-benzene (mCP),[4–8] tetraphenylsilane,[9,10] triazine[11,12] and sterically hindered biphenyl,[13] were developed as high triplet energy cores and modified with a range of functional groups. Hole transport type cores, such as 9-phenylcarbazole, were functionalized with electron transport type units, such as diphenylphosphine oxide, whereas electron transport type cores were substituted with hole transport type substituents, such as carbazole, to obtain the highest occupied molecular orbital (HOMO)/lowest unoccupied molecular orbital (LUMO) levels for bipolar charge transport properties and efficient charge injection. Up to now, the most effective host material for deep blue PHOLEDs was phenylcarbazole derivative modified with diphenylphosphine oxide and a high quantum efficiency of 19.2% was reported.[1]

Other than the core structures mentioned above, dibenzothiophene (DBT) was also reported to be the high triplet energy core structure.[16–19] A DBT compound substituted with diphenylphosphine oxide was applied as an electron transport type exciton blocking layer in blue PHOLEDs and showed good performances.[16,17] This compound was also used as the host material in combination with the hole transport type host material in the double emitting layer structure.[18] The DBT compound was effective in the double layer emitting structure, but the efficiency of the single emitting layer device with the DBT type host was poor due to the strong electron transport properties. On the other hand, the DBT unit can be used as the core structure of high triplet energy materials.

In this study, a series of DBT derivatives with different substituents to manage the charge transport properties were synthesized and high efficiency deep blue PHOLEDs were fabricated using high triplet energy host materials. Substitution of the DBT core with one carbazole and one diphenylphosphine oxide was the most effective in improving the quantum efficiency and efficiency roll-off of deep blue PHOLEDs. High quantum efficiency (>20%) and little efficiency roll-off (<10% of maximum quantum efficiency at 1000 cd m^{-2}) were achieved in the deep blue PHOLEDs using the DBT derivatives. This efficiency is one of the best reported up to now.

Experimental section

Synthesis

The synthetic route of the DBT based host materials is shown in Scheme 1.

Synthesis of 9-(8-bromodibenzo[*b*,*d*]thiophene-2-yl)-9*H*-carbazole (1). 2,8-Dibromo-dibenzothiophene (3.00 g, 8.77 mmol), 9*H*-carbazole (1.76 g, 10.52 mmol), potassium carbonate (5.09 g,

Department of Polymer Science and Engineering, Dankook University, 126, Jukjeon-dong, Suji-gu, Yongin, Gyeonggi, 448-701, Republic of Korea. E-mail: leej17@dankook.ac.kr; Fax: +82 31 8005 3585; Tel: +82 31 8005 3585

† Electronic supplementary information (ESI) available. See DOI: 10.1039/c1jm12421h

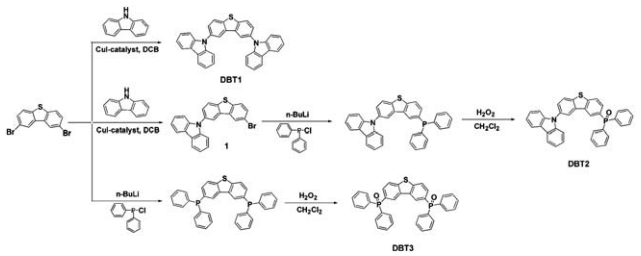

Scheme 1 Synthetic scheme of host materials.

36.84 mmol), copper iodide (0.42 g, 2.19 mmol) and 18-crown-6 (0.23 g, 0.88 mmol) were dissolved in anhydrous *o*-dichlorobenzene under nitrogen atmosphere. The reaction mixture was stirred for 12 h at 100 °C. The mixture was diluted with dichloromethane and washed three times with water (100 mL). The organic layer was dried over anhydrous $MgSO_4$ and evaporated *in vacuo* to give the crude product, which was purified by column chromatography using *n*-hexane as an eluent. The final white powdery product was obtained in 43% yield.

Synthesis of 2,8-di(9*H*-carbazol-9-yl)dibenzo[*b*,*d*]thiophene (DBT1). 2,8-Dibromo-dibenzothiophene (2.00 g, 5.85 mmol), 9*H*-carbazole (2.93 g, 17.54 mmol), potassium carbonate (3.39 g, 24.56 mmol), copper iodide (0.28 g, 1.46 mmol) and 18-crown-6 (0.15 g, 0.58 mmol) were dissolved in anhydrous *o*-dichlorobenzene under a nitrogen atmosphere. The reaction mixture was stirred for 12 h at 100 °C. The mixture was diluted with dichloromethane and washed three times with water (100 mL). The organic layer was dried over anhydrous $MgSO_4$ and evaporated *in vacuo* to give the crude product, which was purified by column chromatography using *n*-hexane as the eluent to afford a white powdery product.

DBT1: yield 43%. T_g 128 °C. ^{1}H NMR (200 MHz, $CDCl_3$): δ 8.31 (s, 2H), 8.17–8.13 (d, 5H), 7.45–7.69 (m, 2H), 7.55–7.24 (m, 13H). ^{13}C NMR (200 MHz, $CDCl_3$): δ 141.2, 139.2, 136.6, 134.9, 126.6, 126.1, 124.4, 123.4, 120.6, 120.4, 120.1, 109.6. MS (FAB) *m*/*z* [(M + H)$^+$] calcd for $C_{36}H_{22}N_2S$ 515.15, found 515. Anal. Calcd for $C_{36}H_{22}N_2S$: C, 84.02; H, 4.31; N, 5.44; S, 6.23. Found: C, 83.39; H, 4.35; N, 5.24; S, 5.80%.

9-(8-(Diphenylphosphoryl)dibenzo[*b*,*d*]thiophene-2-yl)-9*H*-carbazole (DBT2). 9-(8-Bromodibenzo[*b*,*d*]thiophene-2-yl)-9*H*-carbazole (**1**) (1.60 g, 3.74 mmol) in THF (30 mL) was placed into a 100 mL two-necked flask. The reaction flask was cooled to −78 °C and *n*-BuLi (2.5 M in hexane, 1.79 mL) was added dropwise. The whole solution was stirred at this temperature for 3 h, followed by the addition of a solution of chlorodiphenylphophine (0.99 g, 4.48 mmol) in an argon atmosphere. The resulting mixture was warmed gradually to ambient temperature and quenched with methanol (10 mL). The mixture was extracted with dichloromethane. The combined organic layers were dried over magnesium sulfate, filtered, and evaporated under reduced pressure. The white powdery product (1.30 g) was obtained (yield 65%). It was dissolved in dichloromethane (20 mL) and hydrogen peroxide (5 mL), which was stirred overnight at room temperature. The organic layer was separated and washed with dichloromethane and water. The extract was evaporated to dryness to afford a white solid.

DBT2: yield 65%. T_g 115 °C. ^{1}H NMR (200 MHz, $CDCl_3$): δ 8.59–8.53 (d, 1H), 8.30 (s, 1H), 8.18–7.97 (m, 4H), 7.75–7.66 (m, 6H), 7.54–7.31 (m, 12H). ^{13}C NMR (200 MHz, $CDCl_3$): δ 144.6, 141.4, 138.8, 136.7, 135.5, 135.4, 133.3, 132.5, 132.4, 132.2, 130.3, 130.2, 129.7, 129.0, 128.9, 128.7, 127.1, 126.4, 126.3, 124.5, 123.7, 123.5, 123.4, 121.1, 120.7, 120.5, 109.9. MS (FAB) *m*/*z* [(M + H)$^+$] calcd for $C_{36}H_{24}NOPS$ 550.13, found 550. Anal. Calcd for $C_{36}H_{24}NOPS$: C, 78.67; H, 4.40; N, 2.55; S, 5.83. Found: C, 78.78; H, 4.45; N, 2.49; S, 5.59%.

2,8-Bis(diphenylphosphoryl)dibenzo[*b*,*d*]thiophene (DBT3). 2,8-Dibromo-dibenzothiophene (2.50 g, 7.31 mmol) in THF (30 mL) was placed into a 100 mL two-necked flask. The reaction flask was cooled to −78 °C and *n*-BuLi (2.5 M in hexane, 7.30 mL) was added dropwise. The whole solution was stirred at this temperature for 3 h, followed by the addition of a solution of chlorodiphenylphosphine (4.03 g, 18.27 mmol) under an argon atmosphere. The resulting mixture was warmed gradually to ambient temperature and quenched with methanol (10 mL). The mixture was extracted with dichloromethane. The combined organic layers were dried over magnesium sulfate, filtered and evaporated under reduced pressure. The white powdery product was obtained (1.82 g, yield 46%). The powder was dissolved in dichloromethane (20 mL) and hydrogen peroxide (4 mL), and stirred overnight at room temperature. The organic layer was separated and washed with dichloromethane and water. The extract was evaporated to dryness to produce a white solid.

DBT3: yield 46%. T_g 100 °C. ^{1}H NMR (200 MHz, $CDCl_3$): δ 8.50 (s, 1H), 8.44 (s, 1H), 7.99–7.94 (m, 2H), 7.81–7.42 (m, 22H). ^{13}C NMR (200 MHz, $CDCl_3$): δ 143.2, 134.6, 134.4, 132.5, 131.8, 131.8, 131.7, 131.5, 129.9, 129.8, 129.2, 128.4, 128.3, 125.7, 125.6, 122.8, 122.7. MS (FAB) *m*/*z* [(M + H)$^+$] calcd for $C_{36}H_{26}O_2P_2S$ 585.11, found 585. Anal. Calcd for $C_{36}H_{26}O_2P_2S$: C, 73.96; H, 4.48; S, 5.48. Found: C, 73.61; H, 4.47; S, 5.36%.

Device preparation and measurements

DBT1, **DBT2** and **DBT3** were tested as the host materials for blue PHOLEDs. The device structure of the blue PHOLEDs was indium tin oxide (ITO, 150 nm)/*N*,*N*′-diphenyl-*N*,*N*′-bis-[4-(phenyl-*m*-tolyl-amino)-phenyl]-biphenyl-4,4′-diamine (DNTPD, 60 nm)/*N*,*N*′-di(1-naphthyl)-*N*,*N*′-diphenylbenzidine(NPB, 5 nm)/*N*,*N*′-dicarbazolyl-3,5-benzene (mCP, 10 nm)/**DBT1** or **DBT2** or **DBT3**: bis((3,5-difluoro-4-cyanophenyl)pyridine) iridium picolinate (FCNIrpic) (30 nm)/diphenylphosphine oxide-4-(triphenylsilyl)phenyl (TSPO1, 20 nm)/LiF(1 nm)/Al(200 nm). The doping concentration of the FCNIrpic was 15% in all devices. A hole only device with a device structure of ITO/DNTPD (60 nm)/NPB (5 nm)/mCP (10 nm)/**DBT1** or **DBT2** or **DBT3** (30 nm)/DNTPD (5 nm)/Al and an electron only device with a device structure of ITO/TSPO1 (5 nm)/**DBT1** or **DBT2** or **DBT3** (30 nm)/TSPO1 (25 nm)/LiF/Al were also fabricated as single charge devices. All organic materials were evaporated thermally at a vacuum pressure of 8.0×10^{-7} Torr at a deposition rate of 0.1 nm s^{-1} except for the FCNIrpic. All devices were encapsulated with a CaO getter and a glass lid after Al deposition. The device performance of the blue PHOLEDs was measured using a Keithley 2400 source measurement unit and a CS1000 spectroradiometer. Ultraviolet-visible (UV-vis) and photoluminescence (PL)

measurements of the host materials were carried out using 1.0×10^{-4} M tetrahydrofuran solution. Low temperature PL measurements were carried out using a solution of host materials dissolved in tetrahydrofuran under liquid nitrogen. A UV-vis spectrometer (Shimadzu, UV-2501PC) and a fluorescence spectrometer (Hitachi, F-7000) were used to obtain the UV-vis absorption and PL emission data. Cyclic voltammetry was performed using the host films on an ITO substrate in an acetonitrile solution with tetrabutylammonium perchlorate at 0.1 M concentration. Ag was used as the reference electrode and Pt was used as the counter electrode. Ferrocene was used as the standard material for the CV measurement. A potentiostat (Ivium IV) was used to scan the voltage and measure the change in current. The glass transition temperature (T_g) of the host materials was measured using a differential scanning calorimeter (Mettler DSC 822) at a heating rate of 10 °C min^{-1} in a nitrogen atmosphere.

Results and discussion

The DBT core structure has a high triplet energy of 3.01 eV, which is high enough for energy transfer to a deep blue emitting phosphorescent dopant, such as FCNIrpic with a triplet energy of 2.74 eV.[19] The DBT core has electron transport character due to the electron withdrawing sulfur group, which makes the aromatic ring electron deficient. Therefore, DBT was typically used as the high triplet energy core for the electron transport type exciton blocking layer.[16,17] Although DBT was utilized as the core of the exciton blocking layers, the DBT core can also be used as the backbone structure of a high triplet energy host material by controlling the charge transport properties.

DBT was modified with diphenylphosphine oxide and carbazole to tailor the HOMO/LUMO levels and charge transport properties. Diphenylphospine oxide was used as the substituent to improve the electron transport properties,[20] whereas carbazole was introduced to enhance the hole transport properties. Three compounds based on DBT, **DBT1**, **DBT2** and **DBT3**, were synthesized. **DBT1** had two carbazole groups at the 2 and 8 positions of DBT, whereas **DBT3** possessed two diphenylphosphine oxide groups at the 2 and 8 positions. **DBT2** had an asymmetrical molecular structure with one carbazole and one diphenyl phosphine oxide. Scheme 1 shows the synthetic scheme of the host materials. All compounds were synthesized from a 2,8-dibromodibenzothiophene intermediate. The diphenylphosphine oxide unit was substituted to the backbone structure by the lithiation and phosphorylation of the brominated intermediate followed by oxidation with hydrogen peroxide. The carbazole unit was reacted with the brominated intermediate using CuI as a catalyst, yielding the carbazole modified host materials. In the synthesis of asymmetric compound, the carbazole unit was first linked to the core structure followed by diphenylphosphine oxide formation. All compounds were purified by recrystallization and column chromatography to obtain high purity products for device evaluation.

Density functional theory (DFT) calculations of the host materials were carried out using a suite of the Gaussian 09 program to study the molecular orbital distribution. The nonlocal density functional of Becke's 3-parameters employing Lee–Yang–Parr functional (B3LYP) with 6-31G* basis sets was used for the calculation. Fig. 1 shows the simulated HOMO and LUMO distribution of all host materials synthesized in this study. The substituent mostly affected the HOMO distribution of the DBT derivatives and had little effect on LUMO distribution. The DBT core has an electron withdrawing sulfur unit, which makes the aromatic ring electron deficient, inducing LUMO localization in the DBT core. On the other hand, the HOMO is generally localized in the electron donating unit and is heavily affected by the electron donating substituent. The HOMO of **DBT1** with two carbazole moieties was localized mostly over the electron donating carbazole group and the HOMO of **DBT2** was also localized in the carbazole unit. Carbazole is an electron donating unit, inducing localization of the HOMO on the carbazole unit. On the other hand, the HOMO of the **DBT3** was distributed mostly over the dibenzothiophene core due to the strong electron withdrawing properties of the diphenylphosphine oxide. Therefore, it is expected that the HOMO of **DBT3** is shifted downward due to the electron withdrawing character of the dibenzothiophene core. Fig. 1 summarizes the simulated HOMO and LUMO levels. The HOMO of the **DBT3** showed a large value compared to that of **DBT1** and **DBT2**, whereas the LUMO in **DBT3** was not changed greatly. The simulated HOMO of **DBT2** was similar to that of **DBT1** because the HOMO was localized on the same carbazole unit.

The photophysical properties of the host materials were analyzed by UV-vis and PL. Fig. 2 shows UV-vis and PL spectra of the host materials. **DBT1** showed the absorption of the carbazole and dibenzothiophene units, and **DBT2** also exhibited the absorption peaks of the carbazole unit and dibenzothiophene core. The absorption peak at 335 nm corresponds to the π–π* transition of the carbazole moiety, whereas the absorption peaks at short wavelengths were assigned to the absorption of the DBT core. **DBT3** exhibited only the absorption of the π–π* transition of the dibenzothiophene core. The absorption spectra of **DBT1** and **DBT2** were red-shifted compared with that of **DBT3** because of the carbazole centered absorption. The optical band gap could

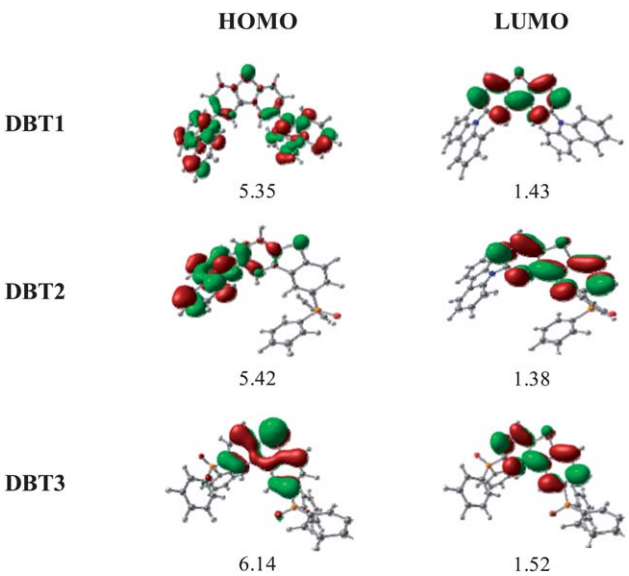

Fig. 1 Molecular simulation results of **DBT1**, **DBT2** and **DBT3**. HOMO and LUMO orbital distribution and simulated energy levels are shown.

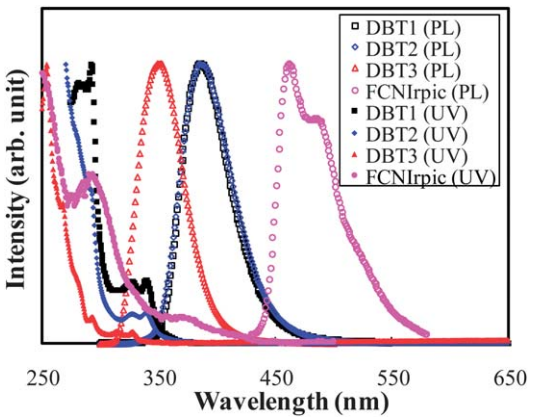

Fig. 2 UV-vis and PL spectra of **DBT1**, **DBT2** and **DBT3**.

be calculated from the absorption edge of the UV-vis spectrum and the band gap of **DBT1** and **DBT2** was 3.52 eV. The band gap of **DBT3** was wider than that of **DBT1** and **DBT2** (3.70 eV). The PL spectrum also showed a similar trend to the UV-vis absorption spectrum. The PL emission was red-shifted in **DBT1** and **DBT2** due to the reduced optical band gap of the host materials. The maximum emission peak of **DBT1** and **DBT2** was 386 nm, whereas that of **DBT3** was 350 nm. The emission spectra of the three host materials were well overlapped with the absorption of the FCNIrpic dopant, indicating that energy transfer from the host materials to the dopant is efficient.

The HOMO levels of the host materials were determined by cyclic voltammetry (CV) (Fig. S1†). The HOMO levels of **DBT1**, **DBT2** and **DBT3** were 6.10, 6.09 and 6.69 eV, respectively. The measured HOMO levels showed a similar trend to the simulated HOMO levels in Fig. 1. The oxidation site of **DBT1** and **DBT2** is the carbazole unit, whereas that of **DBT3** is the dibenzothiophene core. Therefore, similar HOMO levels were observed in **DBT1** and **DBT2**. Table 1 lists the HOMO levels. The LUMO levels could be calculated from the HOMO and optical band gap, and they were 2.58, 2.57 and 2.99 eV for **DBT1**, **DBT2** and **DBT3**, respectively.

The triplet energy of the host materials was measured from a low temperature PL experiment as the peak of PL emission. The triplet energies of the **DBT1**, **DBT2** and **DBT3** were 2.94, 2.92 and 2.96 eV, respectively. All host materials showed a high triplet energy (>2.90 eV) and could effectively transfer energy to the deep blue emitting FCNIrpic dopant material with a triplet energy of 2.74 eV.

Hole only and electron only devices of DBT-based host materials were fabricated to correlate the molecular structure with the charge transport properties of host materials. Fig. 3 shows the hole only and electron only device data of the DBT

Table 1 Photophysical and thermal properties of host materials

	UV-vis[a]/ nm	PL[a]/ nm	HOMO/ eV	LUMO/ eV	Band gap/eV	E_T/ eV	T_g/ °C
DBT1	325, 338	386	6.10	2.58	3.52	2.94	128
DBT2	326, 338	387	6.09	2.57	3.52	2.92	115
DBT3	293, 315, 327	350	6.69	2.99	3.70	2.96	100

[a] Measured in tetrahydrofuran solvent.

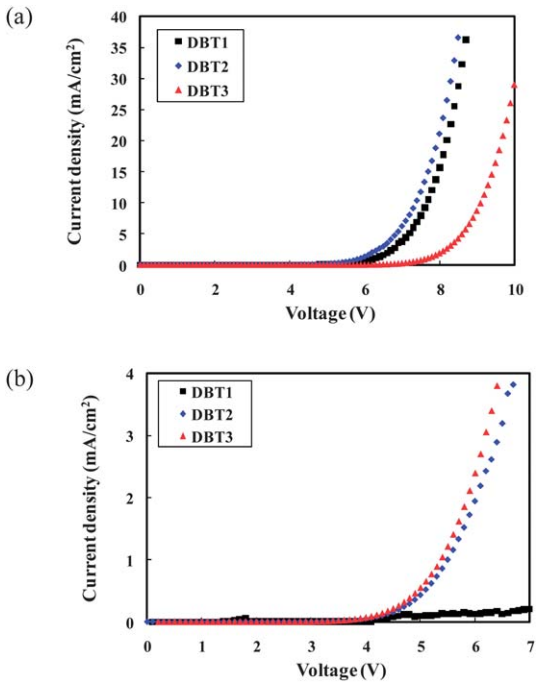

Fig. 3 Hole only (a) and electron only (b) device data of **DBT1**, **DBT2** and **DBT3**.

derivatives. The hole current density was high in the **DBT1** and **DBT2** devices, whereas it was significantly lower in the **DBT3** device. The low hole current density of the **DBT3** device is due to the electron deficient unit in **DBT3**. **DBT3** has an electron deficient dibenzothiophene core and diphenylphosphine oxide substituent. All chemical groups in the **DBT3** have electron withdrawing character, making **DBT3** electron deficient. Therefore, the hole transport properties of **DBT3** are poor. In addition, the HOMO level of 6.69 eV hinders hole injection from the hole transport layer to the **DBT3** host due to the high energy barrier for hole injection of 0.59 eV (hole transport layer HOMO 6.1 eV). The high energy barrier for hole injection and the poor hole transport properties of **DBT3** greatly reduced the hole current density. The high hole current density of **DBT1** and **DBT2** is due to the hole transport carbazole group. The carbazole unit is a good hole transport unit and is effective in improving the hole transport properties of the organic material. The HOMO was dispersed over the hole transport carbazole unit in **DBT1** and **DBT2**, resulting in a high hole current density in **DBT1** and **DBT2**. In addition to the hole transport properties, there was no energy barrier for hole injection in **DBT1** and **DBT2**. The good hole transport properties and little energy barrier for hole injection were responsible for the high hole current density of **DBT1** and **DBT2**.

The electron current density was quite different from the hole current density. **DBT2** and **DBT3** showed much higher current density than **DBT1**. Electron deficient dibenzothiophene and diphenylphosphine oxide in **DBT2** and **DBT3** enhanced the electron transport properties, leading to a high electron current density. On the other hand, the carbazole group in **DBT1** reduced the electron deficiency of the dibenzothiophene core and had a negative effect on the electron current density. A comparison of the hole and electron current densities revealed

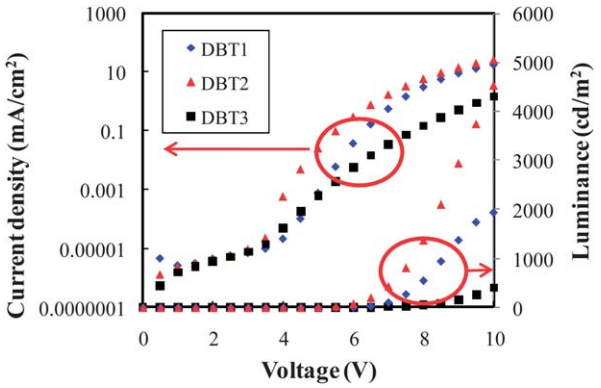

Fig. 4 Current density–voltage–luminance curves of **DBT1**, **DBT2** and **DBT3** devices.

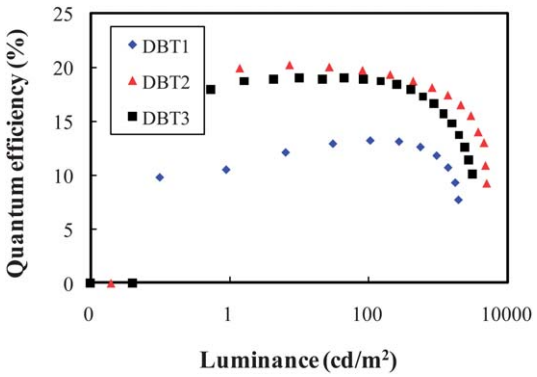

Fig. 5 Quantum efficiency–luminance curves of the deep blue PHOLEDs with the **DBT1**, **DBT2** and **DBT3** host materials.

DBT1 to have strong hole transport properties and **DBT3** to have strong electron transport properties. **DBT2** was similar to **DBT1** for hole transport and to **DBT3** for electron transport. Therefore, it is expected that **DBT2** would be better than **DBT1** and **DBT3** in terms of the holes and electrons balance.

As the DBT type host materials had a high triplet energy for energy transfer to the deep blue phosphorescent dopant, they were evaluated as the host materials for deep blue PHOLEDs. Fig. 4 shows the current density–voltage–luminance curves of the deep blue PHOLEDs with DBT derivatives as the host materials. The deep blue emitting FCNIrpic dopant was doped at a doping concentration of 15% and the device performance was compared. The FCNIrpic has a high triplet energy of 2.74 eV and HOMO/LUMO levels of 5.72/2.98 eV.[21] The **DBT2** device showed higher current density than the **DBT1** and **DBT3** devices. The current density generally depends on the hole and electron densities in the device. Both the hole and electron current densities were high in the **DBT2** hole only and electron only devices, resulting in a high current density in the **DBT2** device. The higher current density of the **DBT1** device was attributed to the high hole current density. The hole current density was much higher than the electron current density and the total current density was dominated by the hole current density. Therefore, the current density of the **DBT1** device was high and slightly lower than that of the **DBT2** device. The current density of the **DBT3** device was low because of the low hole current density despite the high electron current density. The luminance followed the same trend as the current density, even though the luminance of the **DBT1** device was greatly degraded.

Fig. 5 shows the quantum efficiency–luminance curves of the three devices. The **DBT2** device showed higher quantum efficiency than the **DBT1** and **DBT3** devices. As shown in the hole only and electron only devices, **DBT2** exhibited both high hole and electron density. This improves the hole and electron balance in the emitting layer, increasing the quantum efficiency of the **DBT2** device. On the other hand, the hole current density in the **DBT1** device was much higher than the electron density, degrading the holes and electrons balance in the emitting layer. In the case of the **DBT3** device, the charge balance was better than that of the **DBT1** device, resulting in higher quantum efficiency than the **DBT1** device. Nevertheless, the low hole current density of the **DBT3** device could not improve further the quantum efficiency of the **DBT3** device. In particular, the efficiency decrease at high current density was significant due to unbalanced charge injection at high luminance. The maximum quantum efficiency of the **DBT2** device was 20.2% and the quantum efficiency at 1000 cd m^{-2} was 17.7%. There was only about 10% decrease of the quantum efficiency at 1000 cd m^{-2}. The balanced charge injection enhanced the quantum efficiency and suppressed the efficiency roll-off at high luminance. Table 2 lists the performance of all devices. The quantum efficiency of the **DBT2** device is one of the best efficiency values reported for the deep blue PHOLEDs.[21–24] The best quantum efficiency reported in the literature was 25.3%.[21] Although the quantum efficiency of the **DBT2** device was lower than that of the best efficiency value, a high quantum efficiency (>20%) was obtained using the **DBT2** host.

Fig. 6 presents the electroluminescence (EL) spectra of the blue PHOLEDs with the DBT based host materials. All devices showed a main emission peak at 460 nm and a shoulder peak at 479 nm. The main emission peak was not changed depending on the host materials, but the shoulder peak was intensified in the **DBT3** device. **DBT3** is an electron transport type host material and shifts the emission zone from the electron transport layer side to the hole transport layer. The recombination zone shifted to the hole transport layer side induces excimer formation at the interface between the mCP hole transport layer and the **DBT3** host, leading to an intensified shoulder peak at the long wavelength region. The optical effect by the change in recombination zone also increased the intensity of the shoulder peak. The colour coordinates of the **DBT1** and **DBT2** devices at 1000 cd m^{-2} were (0.14, 0.21), whereas those of the **DBT3** device were (0.14, 0.25).

Table 2 Device performances of the blue PHOLEDs with **DBT1**, **DBT2** and **DBT3** hosts

	Maximum quantum efficiency (%)	Quantum efficiency[a] (%)	Color index[b]	Maximum current efficiency/ cd A^{-1}	Maximum power efficiency/ lm W^{-1}
DBT1	13.2	11.5	(0.14, 0.21)	18.2	9.7
DBT2	20.2	17.9	(0.14, 0.21)	28.9	28.9
DBT3	19.0	16.0	(0.14, 0.25)	29.9	17.8

[a] Quantum efficiency was measured at 1000 cd m^{-2}. [b] Color index was measured at 1000 cd m^{-2}.

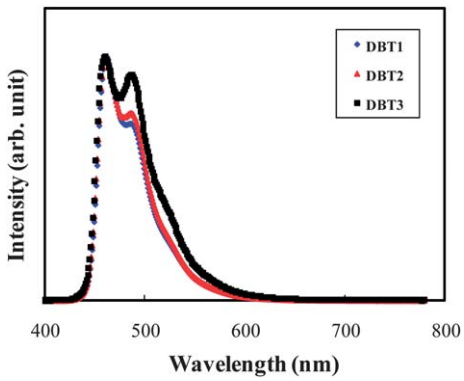

Fig. 6 Electroluminescence spectra of the deep blue PHOLEDs with the **DBT1**, **DBT2** and **DBT3**.

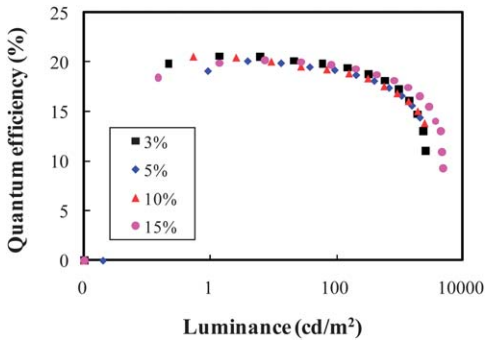

Fig. 7 Quantum efficiency–luminance curves of the **DBT2** devices according to doping concentration.

The device performance of the **DBT2** devices was optimized further by changing the doping concentration of the FCNIrpic dopant. Fig. 7 shows the quantum efficiency of the **DBT2** devices according to the doping concentration. The maximum quantum efficiency of the **DBT2** device was similar over the doping concentration range from 3% to 15%. The doping concentration had little effect on the quantum efficiency, even though the quantum efficiency at high luminance was rather high at high doping concentrations. The bipolar charge transport properties of **DBT2** induced little dependency of the quantum efficiency on the doping concentration. The colour coordinates of the **DBT2** devices were blue-shifted at low doping concentrations and were (0.14, 0.20) at 3% and 5%.

Conclusions

Dibenzothiophene-based host materials with different functional groups were synthesized by modifying the dibenzothiophene with carbazole and diphenylphosphine oxide groups. Holes and electrons were balanced in **DBT2** with a carbazole and a diphenylphosphine oxide, and a high quantum efficiency of 20.2% was achieved. In addition, the efficiency roll-off of the deep blue PHOLEDs was also greatly suppressed. The dibenzothiophene core was proven to be effective as the core structure of high triplet energy host materials.

Notes and references

1 S. O. Jeon, K. S. Yook, C. W. Joo and J. Y. Lee, *Adv. Mater.*, 2010, **22**, 1872.
2 S. O. Jeon, K. S. Yook, C. W. Joo and J. Y. Lee, *Adv. Funct. Mater.*, 2009, **19**, 3644.
3 J. Ding, Q. Wang, L. Zhao, D. Ma, L. Wang, X. Jing and F. Wang, *J. Mater. Chem.*, 2010, **20**, 8126.
4 R. J. Holmes, S. R. Forrest, Y.-J. Tung, R. C. Kwong, J. J. Brown, S. Garon and M. E. Thompson, *Appl. Phys. Lett.*, 2003, **82**, 2422.
5 M. H. Tsai, H. W. Lin, H. C. Su, T. H. Ke, C. C. Wu, F. C. Fang, Y. L. Liao, K. T. Wong and C. I. Wu, *Adv. Mater.*, 2006, **18**, 1216.
6 M. F. Wu, S. J. Yeh, C. T. Chen, H. Murayama, T. Tsuboi, W. Li, I. Chao, S. Liu and J. K. Wang, *Adv. Funct. Mater.*, 2007, **17**, 1887.
7 T. Tsuboi, H. Murayama, S.-J. Yeh, M.-F. Wu and C.-T. Chen, *Opt. Mater.*, 2008, **31**, 366.
8 M. F. Wu, S. J. Yeh, C. T. Chen, H. Murayama, T. Tsuboi, W. Li, I. Chao, S. Liu and J. K. Wang, *Adv. Funct. Mater.*, 2007, **17**, 1887.
9 R. J. Holmes, B. W. D′Andrade, S. R. Forrest, X. Ren, J. Li and M. E. Thompson, *Appl. Phys. Lett.*, 2003, **83**, 3818.
10 X. Ren, J. Li, R. J. Holmes, P. I. Djurovich, S. R. Forrest and M. E. Thompson, *Chem. Mater.*, 2004, **16**, 4743.
11 M. M. Rothmann, S. Haneder, E. D. Como, C. Lennartz, C. Schildknecht and P. Strohriegl, *Chem. Mater.*, 2010, **22**, 2403.
12 K. Son, M. Yahiro, M. T. Imai, H. Yoshizaki and C. Adachi, *Chem. Mater.*, 2008, **20**, 4439.
13 Z. Ge, T. Hayakawa, S. Ando, M. Ueda, T. Akiike, H. Miyamoto, T. Kajita and M. Kakimoto, *Chem. Lett.*, 2008, **37**, 294.
14 F.-M. Hsu, C.-H. Chien, P.-I. Shih and C.-F. Shu, *Chem. Mater.*, 2009, **21**, 1017.
15 S.-J. Su, H. Sasabe, T. Takeda and J. Kido, *Chem. Mater.*, 2008, **20**, 1691.
16 U. S. Bhansali, E. Polikarpov, J. S. Swensen, W.-H. Chen, H. Jia, D. J. Gaspar, B. E. Gnade, A. B. Padmaperuma and M. A. Omary, *Appl. Phys. Lett.*, 2009, **95**, 233304.
17 L. S. Sapochak, A. B. Padmaperuma, P. V. Vecchi, X. Cai and P. E. Burrows, *Proc. SPIE*, 2007, **6655**, 665506.
18 M.-T. Lee, J.-S. Lin, M.-T. Chu and M.-R. Tseng, *Appl. Phys. Lett.*, 2009, **94**, 083506.
19 D. Kim, S. Salman, V. Coropceanu, E. Salomon, A. B. Padmaperuma, L. S. Sapochak, A. Kahn and J. L. Bredas, *Chem. Mater.*, 2010, **22**, 247.
20 A. B. Padmaperuma, L. S. Sapochak and P. E. Burrows, *Chem. Mater.*, 2006, **18**, 2389–2396.
21 S. O. Jeon, S. E. Jang, H. S. Son and J. Y. Lee, *Adv. Mater.*, 2011, **23**, 1436.
22 H. Sasabe, J. Iakamatsu, T. Motoyama, S. Watanabe, G. Wagenblast, N. Langer, O. Molt, E. Fuchs, C. Lennartz and J. Kido, *Adv. Mater.*, 2010, **22**, 5003.
23 H. Seo, K. Yoo, M. Song, J. S. Park, S. Jin, Y. I. Kim and J. J. Kim, *Org. Electron.*, 2010, **11**, 564.
24 H. Son and J. Y. Lee, *Org. Electron.*, 2011, **12**, 1025.